Available online at www.sciencedirect.com

ScienceDirect

IFAC PapersOnLine 52-27 (2019) 163–169

Torque Vectoring for an Electric All-wheel Drive Vehicle

Dávid Mikle, Martin Bať a

Institute of Automotive Mechatronics
Faculty of Electrical Engineering and Information Technology
Slovak University of Technology, Bratislava, Slovakia
(e-mail: david.mikle@stuba.sk, martin.bata@stuba.sk)

Abstract: This paper deals with vehicle dynamics control of an all-wheel drive vehicle. The aim is to design a torque vectoring control system with yaw moment control. Based on theoretical background of basic vehicle drive processes and possible ways of vehicle dynamics control, the control system structure is designed, followed by simulations in Matlab connected to the virtual simulation software CarMaker. Then the control system is ready for implementation into the electronic control unit of formula student type vehicle SGT-FE18, designed and developed by the student team STUBA Green Team.

Keywords: vehicle dynamics; all wheel drive; torque vectoring; vehicle stability

1. INTRODUCTION

A significant challenge in electric vehicles with all-wheel drive is the way to control the individual drives in order to improve vehicle dynamics while increasing safety and stability in cornering. This can be achieved by different control strategies depending on the dynamic response and performance requirement. The most common strategy is yaw rate control. The yaw rate, r [rad/s], is defined as the rotational speed of the car around the z-axis. To create this yaw acceleration the vehicle needs to create a yaw moment M_Z according to (1).

$$M_Z = r \,.\, I_Z \tag{1}$$

where I_Z is moment of inertia.

This momentum can be created in different ways by applying:

1. A steering wheel input
2. Different brake forces
3. A difference in torque between the driven wheels

This paper presents a yaw rate control system based on applying different torque on each wheel, also called torque vectoring (TV). This system is capable to shift torques from the inner to the outer wheels when passing through a corner and reduce or increase torque applied on a wheel depending on driving surface and condition under the wheel. The individual actuation of electric drives allows the continuous generation of the control yaw moment M_Z required to achieve stability in emergency conditions. It also further extends the boundaries of safe vehicle velocities from currently achievable with conventional vehicle stability control systems based only on friction brake actuation or complicated limited slip differentials. This is the biggest advantage of this approach and it ultimately improves the vehicle response.

Typical torque vectoring controllers can be organized on three levels (Fig. 1). The highest control level receives the reference value r_{ref} of vehicle yaw rate, which is calculated from measured or estimated variables, such as the values of steering-wheel angle δ, vehicle longitudinal speed v_x and acceleration a_x. At this control level, feedback controllers are in place for tracking the reference yaw rate. These controllers can be based on PID (Proportional Integral Derivative) control structures (Sakhalkar, 2014), sliding mode approaches (Canale, 2008), linear quadratic regulators (van Zanten, 2000) and (Cheli, 2013), Model Predictive Controllers (MPC) (Falcone, 2007) or robust control (Zhengyi, 2012). In some sources, the feedback controller can be coupled with a feedforward control structure (Cheli, 2009), based on the same inputs (δ, v_x and a_x) adopted for the definition of the reference yaw rate.

At an intermediate level, depending on the number of electric drives, yaw moment calculated by high level controllers is split into different contributions for the individual motors (traction torques or braking torques). This task is addressed by the control allocation strategy that considers a set of constraints including the torque and power limitations of the electric drivetrains, the power limitations of the energy storage unit and the limitations relating to the tire friction ellipse starting from a simplified estimation of the load transfers. The problem of control allocation strategy is addressed by several papers, see e.g. (De Novellis, 2009).

Finally, the lowest layer of a typical torque-vectoring control system consists of torque or current controllers for each electric motor drive.

10.1016/j.ifacol.2019.12.750

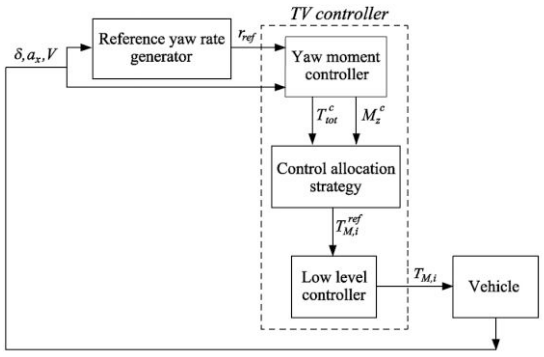

Fig. 1. Typical TV controller layout (De Novellis, 2013).

2. THEORETICAL BACKGROUND

2.1 Vehicle cornering

The first step to design a TV control system, is to analyze the vehicle cornering behavior at very low speeds (< 6kmph). At low speeds, there is no side slip angle of the tires and vehicle turns as shown in Fig. 2. To ensure that wheels roll ideally when cornering, normal of speed vectors of all four wheels must meet at the center of the rotation. This condition can be fulfilled only if the vehicle's theoretical center of rotation O_T lies on the axis of rotation of the rear wheels. Then the front wheels must be steered to angles α and β, so their rotation axes passes through the theoretical center of rotation O_T.

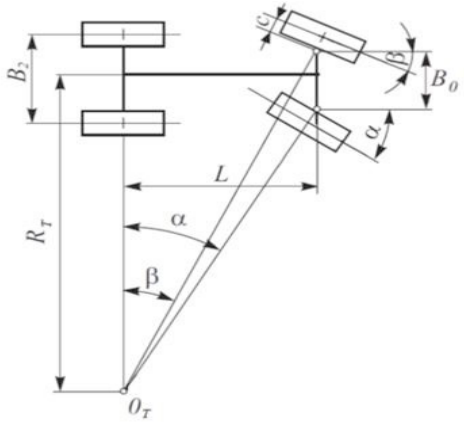

Fig. 2. Vehicle cornering at low speeds.

From the previous figure, following equations can be evaluated.

$$\cot\alpha = \frac{R_T - \frac{B_0}{2}}{L} \tag{2}$$

$$\cot\beta = \frac{R_T + \frac{B_0}{2}}{L} \tag{3}$$

where B_0 is distance between axle joints.

From previous equations, we can determine relation between steering angles.

$$\cot\beta - \cot\alpha = \frac{B_0}{L} \tag{4}$$

This is called Ackerman condition and can be applied only when the car moves at very low speeds. The theoretical radius of rotation R_T can be determined from equations (2) and (3).

$$R_T = \mathrm{L}.\ \cot\alpha + \frac{B_0}{2} = \mathrm{L}.\ \cot\beta - \frac{B_0}{2} \tag{5}$$

$$R_T \cong \mathrm{L}.\ \cot\alpha_A \tag{6}$$

where α_A is the average steering angle of front wheels.

$$\alpha_A = \frac{\alpha + \beta}{2} \tag{7}$$

To analyze the real cornering, we can use a simplified single-track model of vehicle, where the axles are replaced by one wheel in the middle. If we consider driving a car at real speeds (> 6kmph), the centrifugal force F_C produced by center of gravity of vehicle, causes lateral reactions on wheels Y_1, Y_2 with corresponding side slip angles on tires δ_1, δ_2. This results in a change of the radius of rotation from R_T to R_R.

Since the centrifugal force depends on the speed of vehicle and cornering radius, it means that every driving speed will correspond to a different actual radius of rotation. At each given speed, vehicle will therefore turn with the real radius R_R, around the real center of rotation O_R, as shown on figure below.

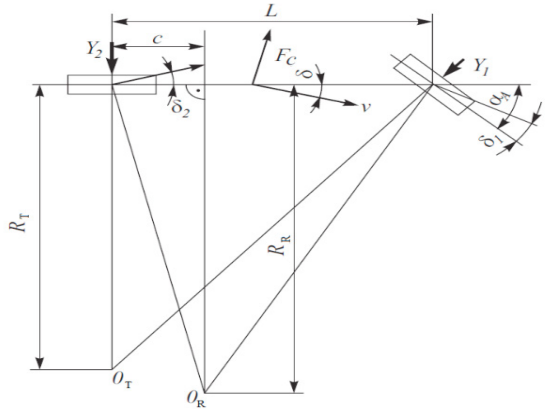

Fig. 3. Single track model of real speeds cornering.

The real cornering radius can be determined as:

$$R_R = \frac{L}{\tan\delta_2 + \tan(\alpha_A - \delta_1)} \tag{8}$$

From equation (8) we can see that R_R doesn't depend only on the steering angle and wheelbase, but also on the side slip angles δ_1, δ_2 (Jazar, 2009), (Irkinský, 1991).

2.2 Vehicle stability

One of the most important features of a car is its stability, not only in terms of driving characteristics and comfort, but especially in terms of safety. In general, the stability of a

vehicle means the ability to maintain a steady state, or return to it without intervention, after any small disturbance.

Vehicle stability can be investigated as:

- Lateral stability - describes movements around the longitudinal axis of vehicle, for example driving on lateral slope.
- Longitudinal stability – describes movements around the lateral axis of vehicle, which can be a result of acceleration and deceleration or driving on a longitudinal slope.
- Directional stability - describes movements around the vertical axis of vehicle, it is a combination of longitudinal and lateral stability in some dynamic states, such as vehicle cornering.

As long as torque vectoring system helps to improve directional stability, possible behaviors of a vehicle while cornering will be furthermore explained (Fig. 4).

Understeering - vehicle has a side slip angle of the front tires greater than rear tires, so the front axle will divert more out of the curve and vehicle turns with a radius greater than the theoretical radius R_T. The real cornering radius R_R will increase as the speed increases.

Oversteering - vehicle has a side slip angle of the rear tires greater than front tires, and therefore the rear axle will divert more out of the curve and vehicle turns with a radius smaller than theoretical radius R_T. As the speed increases, real cornering radius R_R will decrease.

Neutral steering - vehicle has the same side slip angles on front and rear tires and axles will divert in the same way and vehicle turns on the same radius as the theoretical one. This also applies with increasing speed, however vehicle will turn around the real center of rotation O_R, which is only slightly shifted forward in direction of movement (Jazar, 2009), (Ferencey, 2013).

3. CONTROLLER DESIGN

In this paper, vehicle dynamics control problem is solved by implementation of a torque vectoring system, verified by simulations in Matlab. For this purpose, vehicle model is implemented in simulation software IPG CarMaker. When designing the control structure, we wanted to keep the control system as simple as possible, while maintaining the system accuracy with simplifications and calculations used. To achieve this, we will use the theoretical knowledge described in the second chapter of this paper. To ensure neutral steering of vehicle, a torque vectoring control system based on applying different torque on each wheel will be used. The main controlled variable of control system is vehicle yaw rate r. Deviation of r from the reference value r_{ref}, calculated from steering wheel angle, is input to the *Yaw rate controller* block with PID control with feedback loop. This will generate yaw moment M_Z, which should be appropriately distributed to the wheels. This happens in the *Torque distribution* block. The output of it are four reference torques, $T_{ref,xy}$, where xy indicates the wheel's position. The x can be F - front or R - rear and y can be L - left or R- right. Reference torques then enter to *Wheel slip controller* blocks. Wheel slip controller monitors the current wheel slip and keeps it at optimum slip of the tire when the vehicle accelerates. Output from these blocks are four wheel torques T_{xy}, one for each wheel, which directly represent the torque requirements for power inverters of vehicle. In the *Model of vehicle* block, the simulation model of formula student racing car SGT - FE18 is implemented. Controller design is shown in the following figure.

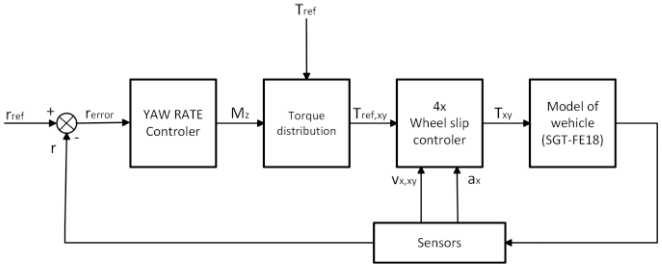

Fig. 5. Controller design.

Finally in the last block *Sensors*, the measurements of following vehicle variables take place:

- Accelerator pedal position
- Steering angle
- Yaw rate
- Longitudinal speed and acceleration
- Wheel speeds

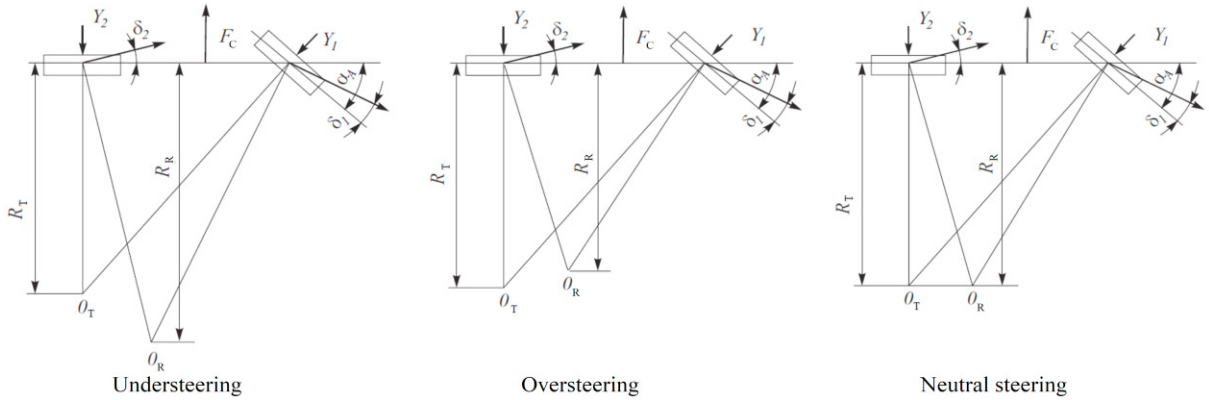

Fig. 4. Vehicle cornering behavior.

3.1 Yaw rate controller

The yaw rate controller contains negative feedback loop, which is implemented by subtracting current yaw rate from reference yaw rate. Since we do not measure reference yaw rate directly, it must be calculated. For this, the general formula for calculating angular velocity is used.

$$\omega = \frac{v}{R} \tag{8}$$

where: ω - angular velocity
v - linear velocity
R - circle radius

For our case we get the following formula.

$$r_{ref} = \frac{v_x}{R_R} \tag{9}$$

To be able to calculate the reference yaw rate, we need to know the real cornering radius R_R. For that, we will use the theoretical background from chapter *Vehicle stability*, where vehicle with a neutral steering steers on the same radius as the theoretical radius R_T. Since aim of a well-designed torque vectoring system is to help vehicle achieve the neutral steering, for further calculations we will consider real cornering radius to be equal to theoretical radius.

$$R_R \cong R_T \cong \mathrm{L}\,.\,\cot\alpha_A \tag{10}$$

The calculation of (10) takes place in block *RT_calc,* where steering angle is used for calculation of α and β and their average α_A is then used for calculation of theoretical radius of rotation. According to equation (9), R_T is then used to calculate a reference yaw rate r_{ref}. By subtracting current yaw rate r from reference we obtain a yaw rate error.

$$r_{error} = r_{ref} - r \tag{11}$$

Implementation of previous equations is shown in the following figure.

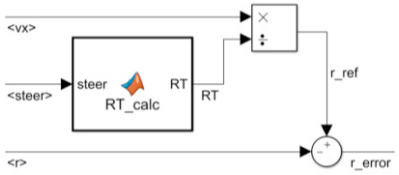

Fig. 6. Calculation of yaw rate error.

Finally, yaw rate error enters to PI controller. Output from it is the yaw moment M_z, which should be then transformed to difference in torques applied on wheels.

3.2 Torque distribution

Input to this block is the yaw moment M_Z, which is appropriately split to the wheels here. In order to be able to adjust distribution of M_Z to front or rear axle, yaw moment distributed to front axle is multiplied by *lambda* and yaw moment distributed to rear axle is multiplied by *lambda* - 1. This means that if *lambda* is equal to 0, M_Z is transferred only to rear axle. If *lambda* is equal to 1, M_Z is transferred only to front axle. And if *lambda* is equal to 0.5, M_Z is transferred equally to both axles.

Next, we need to calculate the traction force to realize the yaw moment. For this, the general formula for calculating angular velocity is used, where the moment M is equal to the force F acting on the lever arm R.

$$M = F\,.R \tag{12}$$

From equation (12) we express the force F and substitute the variables for our case.

$$F = \frac{M}{R} \Rightarrow F_{TT} = \frac{M_Z}{\frac{B_1}{2}} \tag{13}$$

From equation (13) we get total traction force FTT which will apply the needed yaw moment by both axles. However, to calculate the traction force FT for one wheel, we need to divide total traction force by four.

$$F_T = \frac{M_Z}{\frac{B_1}{2}}\frac{1}{4} \tag{14}$$

From equation (14) we get the expression K, which is used in gain block in control structure.

$$F_T = M_Z\frac{1}{\frac{4}{2}B_1} = M_Z\,.K \Rightarrow K = \frac{1}{2\,B_1} \tag{15}$$

If we want the wheel to apply traction force, it is necessary to act on it by traction torque T. We calculate this torque by multiplying F_T by lever arm on which it acts, in our case the dynamic tire radius R_d.

$$T = R_d.F_T = \frac{R_d}{2\,B_1}\,.M_Z \tag{16}$$

The implementation of previous equations is shown in the following figure.

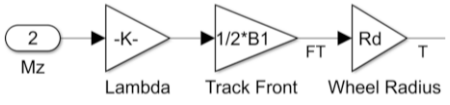

Fig. 7. Calculation of traction torque.

Traction torque is next split to left and right side and added to the torque T_{ref} from accelerator pedal. After this, traction torque passes through saturation block, which acts like anti-windup and shifts oversaturated part of T to opposite wheel of axle. Output from this is the reference torque for each wheel $T_{ref,xy}$ which enters to the four blocks of *Wheel slip controller*. Presented structure is shown in the following figure.

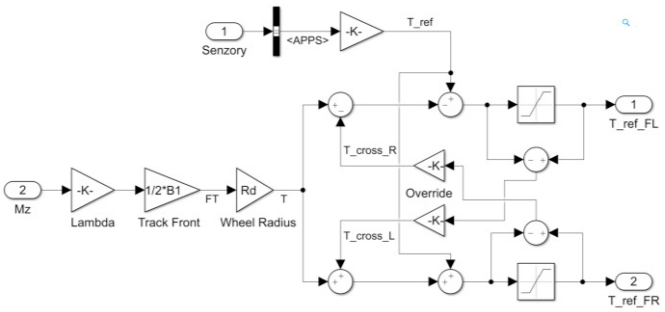

Fig. 8. Torque distribution block

3.2 Wheel slip controller

As mentioned before, four separate wheel slip controller blocks are used, one for each wheel. Their main goal is to monitor the wheel slip and limit the reference moments $T_{ref,xy}$, when wheel slip exceeds optimal slip of tire. For this, actual wheel slip s needs to be calculated according to (17), where v_x is longitudinal speed of vehicle and v_t is tire speed.

$$s = \frac{v_t - v_x}{v_t} \tag{17}$$

By subtracting the actual slip from optimal (reference) slip of tire, we obtain wheel slip error. According to tire documentation from manufacturer Continental, we found out, that the biggest longitudinal force that tire can transfer to road is at wheel slip of 8 – 10%. Note that this differs a lot from conventional tires (20 – 30%), because tiers used on this vehicle are specially developed for formula student competitions.

Calculation of wheel slip error is shown in the following figure.

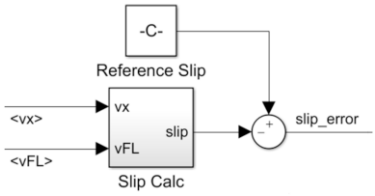

Fig. 9. Calculation of wheel slip error.

Calculated wheel slip error enters to PI controller, output of which is added to the reference torques $T_{ref,xy}$ from *Torque distribution* blocks. Result from them are the torques T_{xy}, which are directly transferred to vehicle model.

3.2 Model of vehicle

As mentioned earlier, vehicle model is implemented in virtual simulation software IPG CarMaker. Vehicle considered here has in-wheel synchronous servo motor drives, each coupled with a single speed, two stage planetary transmission. The main vehicle parameters are stated in Table 1.

Table 1 Main vehicle data.

Overall vehicle mass	235 kg
Wheelbase	1530 mm
Rear track width	1200 mm
Front track width	1210 mm
Height of the vehicle center of gravity	300 mm
Tires	205/470 R13
Maximum electric motor power (each)	35 kW
Maximum electric motor torque (each)	21 Nm
Maximum electric motor speed	20 000 RPM
Transmission gear ratio	13.51:1

4. SIMULATION

To verify designed torque vectoring system, we have built two types of test maneuvers in IPG CarMaker to simulate the dynamic disciplines of formula student competitions. The first maneuver, Skid Pad, consists of two 15.25m circles, in shape of eight (Fig. 10), where vehicle needs to pass circles two times in the clockwise direction and then two times in anticlockwise direction. The aim of this simulation is to verify the functionality of the *Yaw rate controller* as well as *Torque distribution block* and also to verify the stability of the vehicle when cornering.

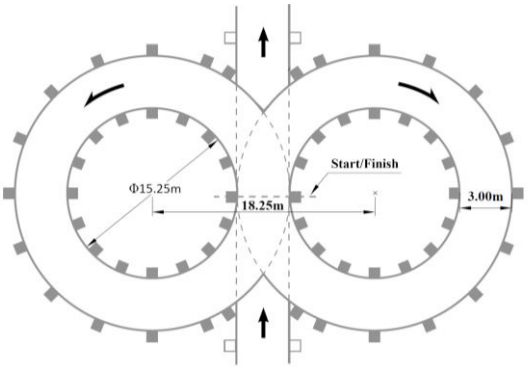

Fig. 10. Skid Pad layout.

We simulated this maneuver for two times. First with the torque vectoring system on, then we deactivate it and repeat the simulation. Results of Skid Pad simulations are shown in the following figures.

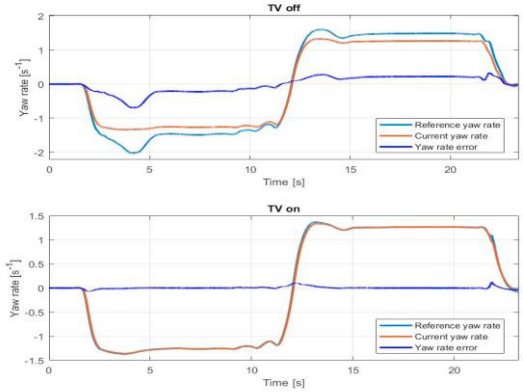

Fig. 11. Yaw rate characteristics with deactivated toque vectoring (TOP) and activated torque vectoring (BOT).

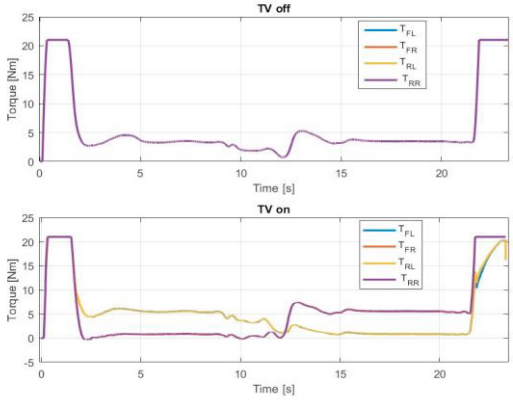

Fig. 12. Torque applied on wheels with deactivated toque vectoring (TOP) and activated torque vectoring (BOT).

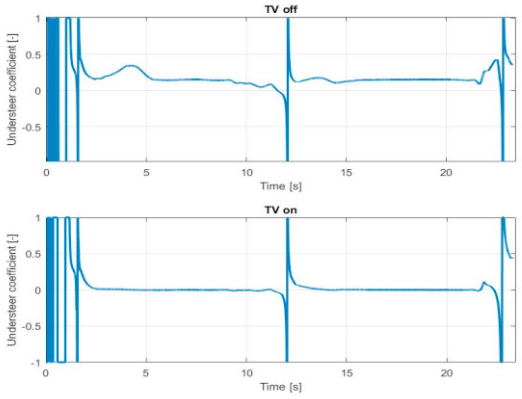

Fig. 13. Understeer coefficient with deactivated toque vectoring (TOP) and activated torque vectoring (BOT).

From Fig. 11 with deactivated torque vectoring system (TV off) we can see that reference yaw rate is significantly greater than the current yaw rate. This means that the driver needs to steer on a greater steering angle to keep the vehicle on the track. Time needed to pass the whole track is 23.418 seconds. The bottom of this figure with activated torque vectoring system (TV on) shows that actual yaw rate is almost identical to reference yaw rate. The resulting time of this simulation is 21.931 seconds, which is almost 1.5 seconds better than in the first case. From Fig. 12 we can see how traction torques are distributed to wheels. In case with TV off are all equal and in case with TV on torques transferred to the outer wheels are greater than torques on inner wheels. Fig. 13 shows the understeer coefficient, which is a variable that tells us what kind of steering behavior vehicle has. If this coefficient is equal to 0, vehicle has neutral steering character, if it is positive, vehicle has understeer behavior and if it's negative, oversteer occurs. We can see that with deactivated TV system, vehicle has significant understeer, while with TV on, vehicle is almost ideally neutral in steady state cornering.

The second dynamic discipline we have simulated is Acceleration. This maneuver simulates acceleration of vehicle from rest to maximum speed. Trajectory of this discipline is a straight track with a length of 80 m, where we can verify the functionality of *Wheel slip controller*. Results of Acceleration simulations are shown in the following figures.

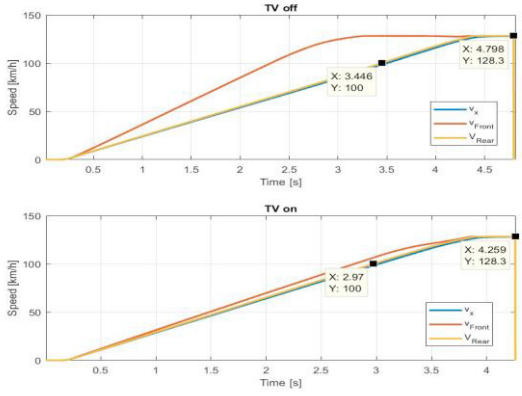

Fig. 14. Vehicle longitudinal speed and wheel speeds characteristics with deactivated toque vectoring (TOP) and activated torque vectoring (BOT).

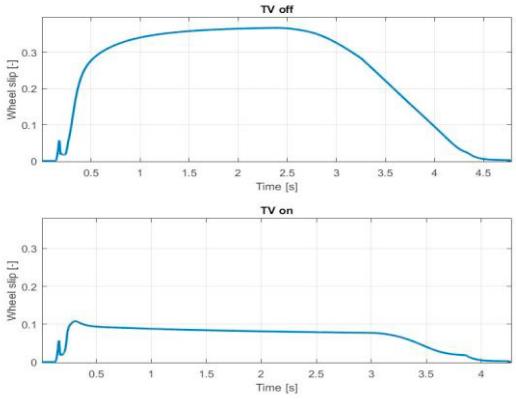

Fig. 15. Wheel slip characteristics with deactivated toque vectoring (TOP) and activated torque vectoring (BOT).

From Fig. 14 we can see that with deactivated torque vectoring system (TV off) front wheels speeds are significantly greater than vehicle speed. This causes an uncontrolled increase of wheel slip that can be seen in Fig. 15. In this case, value of slip reaches almost 40%, which means that tires lost lot of grip and transfer only limited traction force to the road. Time of the acceleration from 0 to 100km/h in this case is 3.446 seconds. However, with activated torque vectoring system, all speeds are very similar to each other, which means that designed wheel slip controller reacted to loss of grip correctly and the torques applied on wheels were limited. In this case, wheel slip remains under 10%, which can be considered as optimal slip, therefore maximum traction force was transferred to road. In this case, acceleration from 0 to 100km/h takes 2.97seconds.

5. CONCLUSION

The paper presents results of simulations and design of torque vectoring control system for formula student type vehicle. For any racecar, the most important objective is to decrease the lap time, which is where the designed system has been found effective, since it significantly helped to vehicle to maintain neutral steering behavior and follow the desired path.

Through the Skid Pad simulation, we tested directional stability of vehicle, verifying the functionality of the Yaw rate controller block, which effectively stabilized vehicle and eliminated any understeer behavior. Through measured characteristic of wheel torques, we verified that the torque distribution block was working properly because it transferred greater torque to the outer wheels, compared with the inner wheels, when cornering.

In addition to this, the vehicle's acceleration performance has been significantly increased by efficient use of available grip on the tires. To verify this feature, we have simulated the acceleration maneuver and verified functionality of the designed wheel slip controller. From the results, we can confirm that the designed controller has significantly improved the vehicle's acceleration capability. Accelerating from 0 to 100 km/h has improved by almost 0.5s, what in motorsport means a high improvement.

Based on the simulation results, we came to conclusion that the designed torque vectoring system works as expected, despite the fact that several simplifications in theoretical background have been used. System is now ready to be implemented to racing car SGT–FE18, shown in following figure.

Fig. 16. SGT-FE18 racing car.

ACKNOWLEDGMENT

The work was supported by the Slovak Research and Development Agency under grant APVV-17-0190.

Also many thanks to IPG Automotive GmbH for support with license and training course for CarMaker simulation software.

REFERENCES

Canale, M., Fagiano, L., Ferrara, A., and Vecchio, C. (2008). Vehicle yaw control via second-order sliding-mode technique. *IEEE Transactions on Industrial Electronics, Vol. 33, No. 11.* pp. 3908-3916.

Cheli, F., Cimatti, F., Dellacha, D. and Zorzutti, A. (2009). Development and implementation of a torque vectoring algorithm for an innovative 4WD driveline for a high-performance vehicle. *Vehicle System Dynamics: International Journal of Vehicle Mechanics and Mobility*, *Vol. 47, No. 2.* pp. 179-193.

Cheli, F., Melzi, S., Sabbioni, E., and Vignati, M. (2013). Torque Vectoring Control of a Four Independent Wheel Drive. In ASME 2013 International Design Engineering Technical Conferences and Computers and Information in Engineering Conference, pp 1–8.

De Novellis, L., Sorniotti, A. and Gruber, P. (2013). Optimal Wheel Torque Distribution for a Four-Wheel-Drive Fully Electric Vehicle. *SAE International Journal of Passenger Cars — Mechanical Systems Vol. 6, No. 1.* pp. 128-136. doi:10.4271/2013-01-0673.

Falcone, P. (2007). Nonlinear model predictive control for autonomous vehicles. PhD thesis, Università del Sannio – Dipartimento di Ingegneria.

Ferencey, V., Vala, M., Bugár, M. (2013). *Mechatronické systémy riadenia dynamiky pohybu automobilov.* 1st edition. 221 p. Slovak University of Technology, Bratislava.

Ikrinský, A., Patek, P., Tichý, J. (1991). *Teória dopravných prostriedkov.* 2nd edition. 294 p. Slovak University of Technology, Bratislava. ISBN 80-227-1318-X.

Jazar R. N. (2009). *Vehicle Dynamics: Theory and Applications.* 1015 p. Springer, New York. ISBN 978-0-387-74243-4.

Sakhalkar, S., Dhillon, P., Kumar, P., Bakshi, S. (2014). Implementation of an Electronic Differential Using Torque Vectoring. 16 p. *SAE Technical Paper* 2014-01-1776, doi:10.4271/2014-01-1776.

van Zanten, A.T. (2000). Bosch ESP Systems: 5 Years of Experience. 11 p. *SAE Technical Paper* 2000-01-1633, doi: 10.4271/2000-01-1633.

Zhengyi H., Xuewu J. (2012). Nonlinear robust control of integrated vehicle dynamics. *Vehicle System Dynamics: International Journal of Vehicle Mechanics and Mobility*, *Vol. 50, No. 2.* pp. 247-280.